DOI: 10.21776/ub.jpacr.2025.014.01.7939 *J. Pure App. Chem. Res.*, **2025**, 14 (1), 23-33
08 April 2025

Design, Synthesis, and In Silico Study of Two *N*-Substituted Pyrazinamide Analogs as Potential Antituberculosis Agents

Muhammad Zulqurnain,[1]* First Ambar Wati,[2] Ana Nurjanah,[1] Layli Adha Nadira Kavin,[2] Rizqi Nur Afifah,[2] Suyatno Sutoyo,[2] and Mardi Santoso[3]

[1]Department of Chemistry, Faculty of Mathematics and Natural Sciences, Universitas Bakti Indonesia, Jalan Kampus Bumi Cempokosari No.40, Cluring District, Banyuwangi Regency, East Java 68482, Indonesia
[2]Department of Chemistry, Faculty of Mathematics and Natural Sciences, Universitas Negeri Surabaya, Ketintang, Gayungan District, Surabaya, East Java 60231, Indonesia
[3]Department of Chemistry, Faculty of Analytical Data Science, Institut Teknologi Sepuluh Nopember, Kampus ITS Sukolilo, Surabaya, East Java 60111, Indonesia

*Corresponding email : zulqurnain.chemistry@gmail.com

Received 24 February 2025; Accepted 30 March 2025

ABSTRACT

Tuberculosis (TB) is an infectious yet often overlooked disease that remains a significant global challenge. Pyrazinamide (PZA), a key drug in the first-line TB treatment regimen, is used to reduce the duration of therapy, making it a compound of great interest for further exploration. Two pyrazine-2-carboxamide analogs have been successfully synthesized and reported, followed by an in-silico evaluation of their potency as antituberculosis agents. Yamaguchi reagent was employed as a coupling agent between pyrazine-2-carboxylic acid and corresponding amine, yielding *N*-(cyclohexylmethyl) pyrazine-2-carboxamide **(D)** and *N*-(4-cyclooctyl) pyrazine-2-carboxamide **(E)** in 60% and 55%, respectively. The molecular docking analysis of compounds **(D)** and **(E)** demonstrated lower binding energies (-7.65 and -7.37 kcal/mol, respectively), in comparison with the standard TB drugs, pyrazinamide and isoniazid. Additionally, ADME and pharmacokinetics evaluations revealed that compounds **(D)** and **(E)** meet the essential criteria for oral drug candidacy. These findings suggest that the pyrazinamide analogs **(D)** and **(E)** hold significant potential as promising antimycobacterial agents for tuberculosis therapy.

Key word: pyrazinamide, yamaguchi-reaction, antituberculosis, molecular-docking, ADME-study

INTRODUCTION

Tuberculosis (TB) continues to pose a major challenge to global health. This contagious illness, triggered by Mycobacterium tuberculosis, predominantly impacts the lungs but is also capable of affecting other organs [1]. TB continues to rank among the top ten of causing death in the world. Based on the recent World Health Organization (WHO) reports, Indonesia belongs to the 30 countries with the most prominent TB burden. In 2022, Indonesia ranked second after India in terms of TB cases. The situation in Indonesia is further exacerbated by the rise multidrug-resistant tuberculosis (MDR-TB), with approximately 75% of TB cases in Indonesia exhibiting MDR-TB between 2016 and 2021 [2].

The development of MDR-TB is often associated with the prolonged duration of TB treatment, leading to poor patient adherence. Standard TB therapy involves administering four primary drugs-pyrazinamide (PZA), isoniazid (INH), rifampicin, and ethambutol [3,4]. The

The journal homepage www.jpacr.ub.ac.id
p-ISSN : 2302 – 4690 | e-ISSN : 2541 – 0733

lengthy treatment period frequently reduces patient compliance, contributing to the existence of drug resistance. Consequently, there is a pressing necessity to develop new antituberculosis drugs with shorter treatment durations and enhanced efficacy.

Pyrazinamide is a crucial first-line drug that effectively inhibits *M. tuberculosis*, particularly in its semidormant state. This heterocyclic aromatic compound has been utilized for over 50 years to shorten the treatment of TB which was from 9–12 months to six months by targeting bacterial populations in acidic environments resistant to other TB drugs. Research has demonstrated that pyrazinamide analogs with specific structural modifications, particularly *N*-substituents on the pyrazine ring, exhibit strong antibacterial activity. The results serve as a basis for the development of pyrazinamide analogs as potential candidates for novel antituberculosis drugs [5-11].

Modifying pyrazinamide's chemical structure has been one of the recent attempts to enhance the bioactivity. Prior studies revealed that pyrazinamide analogs without substituents on the pyrazine ring, as well as those with *N*-substituents such as cyclohexylmethyl and cyclohexyloctyl groups, demonstrate high bioactivity against *M. tuberculosis* [12-15]. Based on these findings, the current research aims to study for the synthesis, in silico ADME studies, and molecular docking analysis of two pyrazinamide analogs, namely *N*-(cyclohexylmethyl)pyrazine-2-carboxamide **(D)** and *N*-(4-cyclooctyl)pyrazine-2-carboxamide **(E)**, as illustrated in Figure 1.

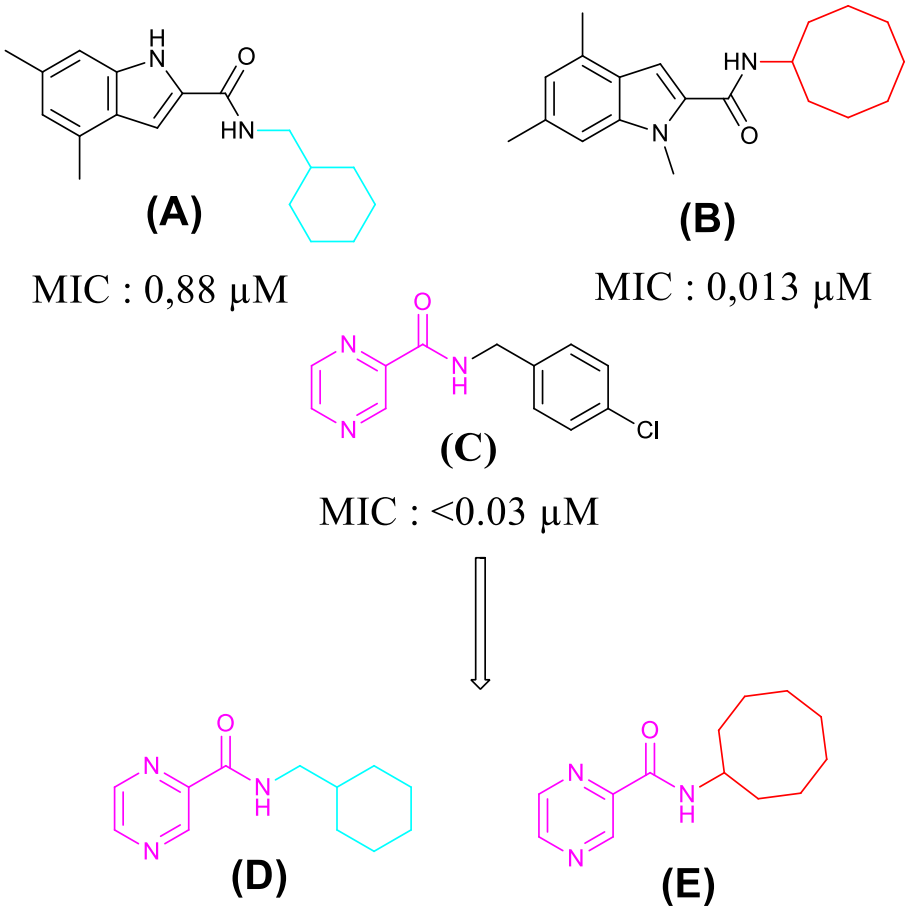

Figure 1. Modification of pyrazinamide analog compounds

The journal homepage www.jpacr.ub.ac.id
p-ISSN : 2302 – 4690 | e-ISSN : 2541 – 0733

Traditional methods for synthesizing pyrazinamide analogs often involve thionyl chloride, which poses significant safety and environmental concerns due to its toxic sulfur dioxide by product. To address these limitations, the Yamaguchi reaction has been proposed as an alternative synthesis route. This method involves the use of 2,4,6-trichlorobenzoyl chloride and triethylamine in tetrahydrofuran, followed by refluxing with dimethyl aminopyridine in toluene. The Yamaguchi reaction facilitates a one-pot amidation process, offering a safer and more efficient approach for synthesizing pyrazinamide analogs [16,17]. Based on this approach, compounds **(D)** and **(E)** will be synthesized using the Yamaguchi reaction method.

EXPERIMENT

Chemicals and instrumentation

All chemicals were bought from manufacturer and directly used or as mentioned include pyrazine-2-carboxylic acid (99% purity, Sigma P56100), cyclohexyl methylamine (98% purity, Sigma 101842), cyclooctylamine (purity >98% (GC), TCI C1223), 4-dimethylaminopyridine (for synthesis, Merck 8.20499.0025), triethylamine (for synthesis, Merck 8.08352.1000), 2,4,6-trichlorobenzoyl chloride (purity 97%, Sigma 345504), tetrahydrofuran (purity ≥ 99.8% (GC), Merck 1.09731.2500), sodium hydroxide (pellets pure, Merck 106462), sodium bicarbonate (for analysis, Merck 106329), hydrochloric acid 37%, and magnesium sulfate heptahydrate (for analysis, Merck 105886). Solvents employed for radial chromatography were distilled technical grade. Reaction monitoring was carried out using thin-layer chromatography. Purification utilizing a radial chromatography employed silica gel 60 PF254 blended with gypsum. Several instruments that were utilized for analysis included melting point (Fisher-John apparatus), Fourier Transform Infrared Spectroscopy (FTIR, Bruker Alpha II FTIR equipped with ATR), Nuclear magnetic resonance (NMR, JEOL Resonance or an Agilent), and Liquid Chromatography-Mass Spectrometry (LCMS/MS Xevo G2-QTOF-MS/MS).

Procedure reaction (Synthesis of pyrazinamide analogs (D) and (E))

The synthesis method was adapted from our previously reported procedure [14]. To the 20 mL of tetrahydrofuran (THF) were added pyrazine-2-carboxylic acid **(F)** (0.81 mmol), triethylamine (0.77 mmol), 2,4,6-trichlorobenzoyl chloride (TCBC) **(G)** (0.77 mmol), 4-dimethylaminopyridine (DMAP) (0.77 mmol) and corresponding amines **(H**, **I)** (0.77 mmol), and refluxed for about 4 – 5 hours. TLC was used to monitor the reaction. After the completion, the mixture was left to room temperature (approximately 25°C) prior to filtration. The obtained filtrate was added with cold water and dichloromethane for extraction. The organic phase was subsequently extracted with HCl 5%, NaOH 5%, $NaHCO_3$ 5%, and aqua. Next, the organic phase was added with anhydrous magnesium sulfate, filtered, and evaporated under vacuo to obtain the desired product, which then need purifying by chromatotron (radial chromatography). Ethyl acetate:*n*-hexane (1:6) was utilized as mobile phase for the purification of both compounds **(D, E).**

ADME screening

ADME properties were screened using the SwissADME tool, developed by the Swiss Institute of Bioinformatics (https://www.sib.swiss, accessed on December 26, 2024). This platform integrates advanced computational methodologies, including multiple linear

The journal homepage www.jpacr.ub.ac.id
p-ISSN : 2302 – 4690 | e-ISSN : 2541 – 0733

regression, binary classification, and support vector machine (SVM) algorithms. These techniques are applied to extensive datasets comprising previously characterized compounds, categorized as inhibitors or non-inhibitors, and substrates or non-substrates. By leveraging these robust models, SwissADME enables accurate prediction of pharmacokinetic and physicochemical profiles critical for early drug discovery processes [18].

Molecular docking

The three-dimensional structure of the InhA enzyme from *M. tuberculosis* in complex with (3S)-1-cyclohexyl-*N*-(3,5-dichlorophenyl)-5-oxopyrrolidine-3-carboxamide **(641)** was retrieved from the Protein Data Bank (PDB ID: 4TZK). Receptor preparation was performed using AutoDockTools version 1.5.6 by removing all crystallographic water molecules, adding polar hydrogens, and assigning Kollman charges to ensure proper receptor geometry for docking.

Ligand structures, including *N*-(cyclohexylmethyl) pyrazine-2-carboxamide **(D)**, *N*-cyclooctylpyrazine-2-carboxamide **(E)**, pyrazinamide **(PZA)**, and isoniazid **(INH)**, were constructed as 2D molecular representations using MarvinSketch version 24.1.3. Energy minimization was applied to all ligands using the MMFF94 (Merck Molecular Force Field) optimization tool integrated into MarvinSketch to achieve stable conformations.

Molecular docking simulations were conducted using AutoDock 4.2.6 [19]. The binding site of the InhA enzyme was defined by centering the grid box at coordinates x: 10.119, y: 32.370, and z: 60.728. The grid dimensions were set to 32 × 26 × 22 Å in xyz axes, ensuring sufficient coverage of the active site. The Lamarkian genetic algorithm was employed as the search method with 100 independent genetic algorithm runs to explore potential binding conformations of the ligands within the receptor's active site. Docking results, including binding energies and interactions, were examined and depicted using Biovia Discovery Studio Visualizer (© 2024), which provided detailed insights into the ligand-receptor binding poses and interactions.

RESULT AND DISCUSSION

Synthesis and characterization of pyrazinamide analogs (D and E)

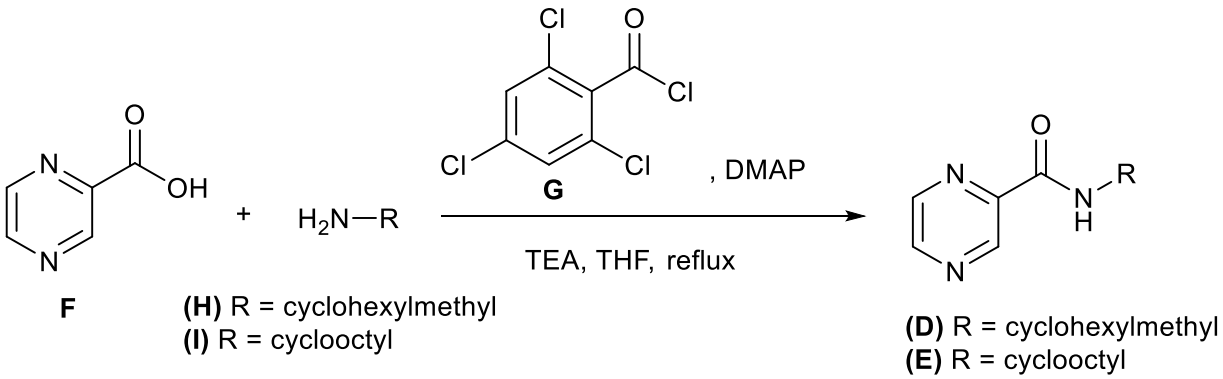

Figure 1. Synthesis of pyrazinamide analogs *N*-(cyclohexylmethyl)pyrazine-2-carboxamide **(D)** and *N*-(4-cyclooctyl)pyrazine-2-carboxamide **(E)**

Yamaguchi reagent was firstly used for esterification, then later applied for thioester formation [20,21]. Synthesis of two pyrazinamide analogs, *N*-(cyclohexylmethyl)pyrazine-2-carboxamide **(D)** and *N*-(4-cyclooctyl)pyrazine-2-carboxamide **(E)**, adapted from the our

The journal homepage www.jpacr.ub.ac.id
p-ISSN : 2302 – 4690 | e-ISSN : 2541 – 0733

previously reported method [14]. A detailed description of the reaction mechanism involved in the synthesis of pyrazinamide analogs is shown in Figure 1. The reaction was conducted by the addition of triethylamine (TEA) as protonating agent to the solution of pyrazine-2-carboxylic acid in tetrahydrofuran (THF) to form pyrazine-2-carboxylic anion. The anion attacked 2,4,6-trichlorobenzoyl chloride **(G)** to produce mixed anhydride which was further treated with 4-dimethylaminopyridine (DMAP) catalyst and corresponding aliphatic amines **(H, I)** under reflux condition for 4 – 5 hours. The obtained mixture was filtered off, and the filtrate was extracted with dichloromethane, subjected to repetitive washing of 5% HCl, 5% NaOH, 5% $NaHCO_3$, and water. The crude extract was obtained after evaporation under low pressure which later was purified by chromatotron to obtain pure product **(D)** and **(E)** at 0.101 g (yield 60%) and 0.099 g (yield 55%), in respectively. Melting point of synthesized compounds were 93.8 – 94°C for **(D)** and 103.8 – 104°C for **(E)**.

Table 1. ^{1}H-NMR data of pyrazinamide analogs

Proton	Chemical shift (δ) (in $CDCl_3$, ppm)	
	N*-(cyclohexylmethyl)pyrazine-2-carboxamide (D)	***N*-cyclooctylpyrazine-2-carboxamide (E)****
-CH_2-	0.95-1.03 (m, 2H)	1.59-1.73 (m, 12H)
	1.12-1.27 (m, 4H)	1.91-1.97 (m, 2H)
	1.54-1.75 (m, 5H)	
	3.31 (t, *J*= 6.6 Hz, 2H)	
-CH-	*Overlapping*	4.21 (qt, 1H)
ArH	8.51 (s, 1H)	8.50 (dd, *J*= 2.5; 1.6 Hz, 1H)
	8.72 (s, 1H)	8.73 (d, *J*= 2.5 Hz, 1H)
	9.39 (s, 1H)	9.40 (d, *J*= 1.6 Hz, 1H)
NH	7.87 (bs, 1H)	7.77 (bs, 1H)

*Measured in ^{1}H-NMR 400 MHz; **Measured in ^{1}H-NMR 500 MHz

Table 2. ^{13}C-NMR data of pyrazinamide analogs

Carbon	Chemical Shift (δ) (in $CDCl_3$, ppm)	
	N*-(cyclohexylmethyl)pyrazine-2-carboxamide (D)	***N*-cyclooctylpyrazine-2-carboxamide (E)****
-CH_2-	25.9	23.8
	26.4	25.5
	30.9	27.3
	45.7	32.2
-CH-	38.1	49.6
ArCH	142.7	142.5
	144.4	144.5
	147.1	147.1
ArC	144.8	145.0
C=O	163.0	161.8

*Measured in ^{13}C-NMR 100 MHz; **Measured in ^{13}C-NMR 125 MHz

The journal homepage www.jpacr.ub.ac.id
p-ISSN : 2302 – 4690 | e-ISSN : 2541 – 0733

Characterization of ESI high resolution mass spectrometry (ESI-HRMS) resulted on the detected species of pyrazinamide analogs **(D, E)** which was $[M+H]^+$ **(D)** calculated 220.1450, found 220.1452; **(E)** calculated 234.1606, found 234.1609). Furthermore, the IR spectra of **(D)** and **(E)** displayed characteristic carbonyl group absorptions at 1667.61 cm^{-1} and 1657.28 cm^{-1}, respectively. The secondary N-H group absorptions appeared at 3369.33 cm^{-1} **(D)** and 3365.06 cm^{-1} **(E)**, confirming that both compounds were obtained as amides. ^{1}H-NMR was recorded in $CDCl_3$, and the data confirmed the structure of **(D)** and **(E)**. It showed broad singlet (bs) signal at δ 7.77 and 7.87 in **(D)** and **(E)**, in respectively, that indicated the emergence of N-H proton. It was also supported by the ^{13}C-NMR data, giving carbonyl (C=O) signal at δ 161.8 for **(D)** and 163.0 for **(E)**. The details can be seen at Table 1 for ^{1}H-NMR data and Table 2 for ^{13}C-NMR data.

ADME Screening Results

The pharmacokinetic characteristics, including absorption, distribution, metabolism, and excretion (ADME), of two novel pyrazinamide analog compounds **(D)** and **(E)** were evaluated using in silico approaches. The physical characteristics of the synthesized compounds were compared to those of commercially available tuberculosis drugs, focusing parameters such as molecular weight (MW), topological polar surface area (TPSA), hydrogen bond acceptors (HBA), hydrogen bond donors (HBD), Moriguchi's logP (MlogP), and water solubility [22]. This data is summarized in Table 3. The results indicated that both compounds have molecular weights within the recommended range of 160–480 g/mol. This range is associated with lower bioavailability, limited absorption fractions, and a higher binding tendency [22]. TPSA, as one of the primary physicochemical parameters, was employed to predict the absorption potential of the molecules. Previous studies have demonstrated that molecules with TPSA > 140 $Å^2$ exhibit low membrane permeability, whereas those with TPSA < 60 $Å^2$ display better biological membrane penetration [23]. All synthesized compounds exhibited good water solubility. Lipophilicity, measured as LogP, is a key parameter for estimating the oral viability of a drug. Pharmaceutical molecules with LogP values within the range of 0–5 are considered ideal [22]. In this study, both compounds showed LogP values of 0.87, which fall within the optimal range for biological membrane penetration.

Table 3. Chemical properties of the compounds.

Compound	MW (g/mol)	TPSA ($Å^2$)	HBA	HBD	Rotatable Bonds	Moriguchi's LogP	Water Solubility
D	219.28	54.88	3	1	4	0.60	Soluble
E	233.31	54.88	3	1	3	0.87	Soluble
PZA	123.11	68.87	3	1	1	-1.66	Soluble
INH	137.14	68.01	3	2	2	-0.47	Soluble

The evaluation of drug-likeness was conducted using Lipinski's "Rule of Five," Ghose filters, and Veber criteria. The synthesized compounds displayed ADMET profiles that qualify them as potential oral drug candidates, as summarized in Table 4. From a pharmacokinetic perspective, all compounds demonstrated high gastrointestinal absorption. Additionally, both compounds were predicted to cross the blood-brain barrier (BBB), as indicated by a "Yes" result in the BBB permeability predictions. The ability to penetrate the BBB is a critical parameter, particularly in the development of drugs targeting diseases involving the central

The journal homepage www.jpacr.ub.ac.id
p-ISSN : 2302 – 4690 | e-ISSN : 2541 – 0733

nervous system, such as cerebral tuberculosis. However, the ability to penetrate the BBB also poses a potential risk of central nervous system side effects if the compounds exhibit toxicity [24]. Therefore, further analyses are necessary to ensure the safety of the molecules concerning brain tissue interactions. The interaction of the compounds with cytochrome P450 (CYP) enzyme isoforms was evaluated to predict potential side effects or hepatotoxicity risks [25]. Computational analysis of CYP enzyme inhibition, focusing on isoforms CYP1A2, CYP2C19, CYP2C9, CYP2D6, and CYP3A4, demonstrated that compound **(E)** selectively inhibits the CYP1A2 isoform. This selective inhibition suggests a low risk of adverse effects or toxicity related to other CYP enzymes. Consequently, the two newly synthesized pyrazinamide analogs present favorable ADMET profiles, highlighting their potential as drug candidates for tuberculosis therapy. However, further experimental investigations are essential to confirm their pharmacological efficacy and safety for clinical applications.

Table 4. Pharmacokinetics and drug-likeness prediction.

Compound	GI Absorbtion	BBB Perm.	P-gp Substrat	CYP1A2 Inhib.	CYP2C19 Inhib.	CYP2C9 Inhib.	CYP2D6 Inhib.	CYP3A4 Inhib.	Log Kp (cm/s)	Lipinski	Ghose	Veber	Bio. Score
D	high	yes	no	no	no	no	no	no	-5.96	yes	yes	yes	0.55
E	high	yes	no	yes	no	no	no	no	-6.10	yes	yes	yes	0.55
PZA	high	no	no	no	no	no	no	no	-7.48	yes	no:4 viol.	yes	0.55
INH	high	no	no	no	no	no	no	no	-7.63	yes	no:3 viol.	yes	0.55

Molecular docking studies

Molecular docking studies of molecules **(D)** and **(E)** were conducted targeting the inhibition of InhA (PDB: 4TZK). Validation was performed using a grid box with dimensions of 32 × 26 × 22 and a grid center at coordinates (10.119, 32.370, 60.728). The validation yielded a root mean square deviation (RMSD) value of 1.14 Å, indicating a close resemblance between the original ligand structure and the validated ligand structure. Validation is deemed successful if the RMSD value is less than 2 Å, demonstrating that the protocol used can reliably replicate the native ligand-receptor interactions [14]. The similarity between the original ligand and the validated ligand is shown in Figure 2.

Redocking of the ligand (3S)-1-cyclohexyl-*N*-(3,5-dichlorophenyl)-5-oxopyrrolidine-3-carboxamide **(641)** with InhA resulted in a binding energy of -11.1 kcal/mol. As depicted in Figure 3, the ligand **(641)** forms interactions with key amino acid residues. Hydrogen bonds were observed between the oxygen atom of the pyrrolidine carbonyl group and Tyr 158 as well as NAD 500 [26]. The cyclohexyl substituent forms an alkyl interaction with Met 161. Additionally, the aromatic phenyl ring establishes several hydrophobic interactions, including π-σ interactions with Ile 215 and π-alkyl interactions with Ala 157. Furthermore, the two chlorine atoms substituted on the phenyl ring contribute to hydrophobic interactions through alkyl contacts with several amino acid residues, such as Leu 218, Met 155, Ile 202, Leu 207, Met 103, and Ala 157 [27].

The journal homepage www.jpacr.ub.ac.id
p-ISSN : 2302 – 4690 | e-ISSN : 2541 – 0733

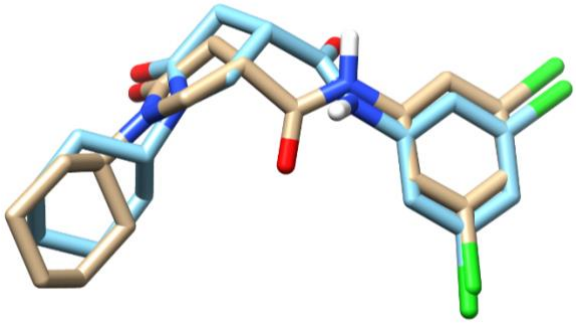

Figure 2. Comparison of the original ligand 641 structure from crystallography with the validated docking model.

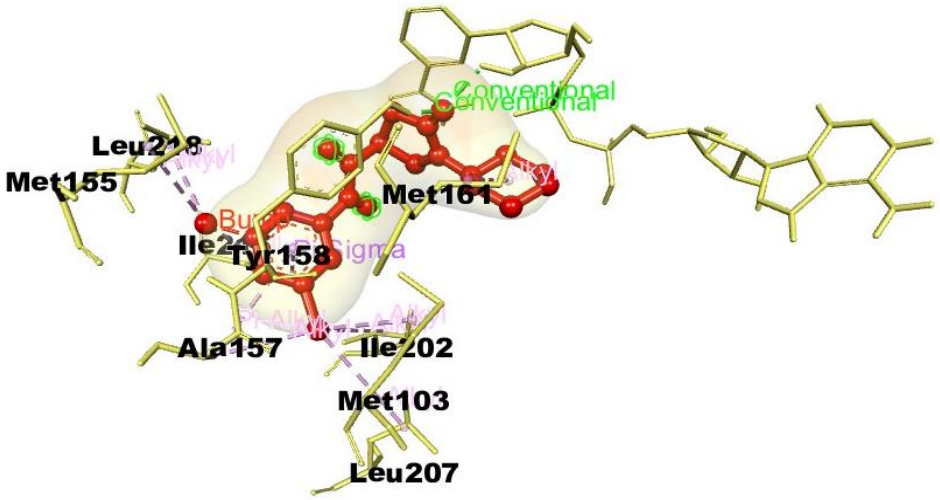

Figure 3. 3D Visualization of the Redocking Results for Ligand **(641)**

Molecular docking analysis revealed that compound **(D)** achieved the most favorable binding energy of -7.65 kcal/mol. As presented in Table 5, both compounds **(D)** and **(E)** interact with the key amino acid residues Tyr 158 and NAD 500 through hydrogen bonds, which are essential for InhA inhibition [22]. In contrast, for compound **(E)**, the hydrogen bonds with Tyr 158 and NAD 500 occur through the oxygen atom of the carbonyl group in the amide, serving as the hydrogen bond acceptor. The pyrazine ring in compound **(E)** also interacts electrostatically with NAD 500 via a π-cation interaction, resulting from the strong attraction between the positively charged NAD 500 and the π-electron cloud of the pyrazine ring [28]. For compound **(D)**, the pyrazine ring forms hydrophobic interactions with Met 161 through alkyl bonding, while the *N*-cyclohexylmethyl substituent engages in π-alkyl interactions with residues Ala 157, Leu 218, Met 155, and Ile 215. Conversely, compound **(E)** forms fewer hydrophobic interactions, interacting only with four residues: Met 199, Phe 149, Leu 218, and Ile 215 (Figure 4). The increased number of hydrophobic interactions in compound **(D)** contributes to stronger binding with InhA, resulting in a more favorable binding energy and more efficient interaction with InhA compared to compound **(E)**.

The journal homepage www.jpacr.ub.ac.id
p-ISSN : 2302 – 4690 | e-ISSN : 2541 – 0733

Table 5. Molecular docking results

Compound	Binding Energy (kcal/mol)	RMSD (Å)	Type of Interaction		
			Hydrogen bond	Hydrophobic interaction	Electrostatic interaction
D	-7,65	73,5	Tyr 158, NAD 500	π-π T-shaped: Tyr 158 Alkyl: Met 161 π-alkyl: Ala 157, Leu 218, Met 155, Ile 215	-
E	-7,37	72,02	Tyr 158, NAD 500	Alkyl: Met 199 π-alkyl: Met 199, Phe 149, Leu 218, Ile 215	π-cation: NAD 500 π-anion: Phe 149
641	-10,93	1.14	Tyr 158, NAD 500	π-π T-shaped: Tyr 158 Alkyl: Met 103, Leu 207, Ala 157, Met 161, Met 155, Ile 215 Leu 218 π-alkyl: Ala 157 π-σ: Ile 215	-
PZA	-4,51	69,07	NAD 500, Lys 165	π-π T-shaped: Tyr 158 π-alkyl: Met 199, NAD 500	-
INH	-4,81	67,48	Tyr 158, NAD 500	π-π T-shaped: Phe 149 π-alkyl: Met 199, NAD 500	π-lone pair: Phe 149

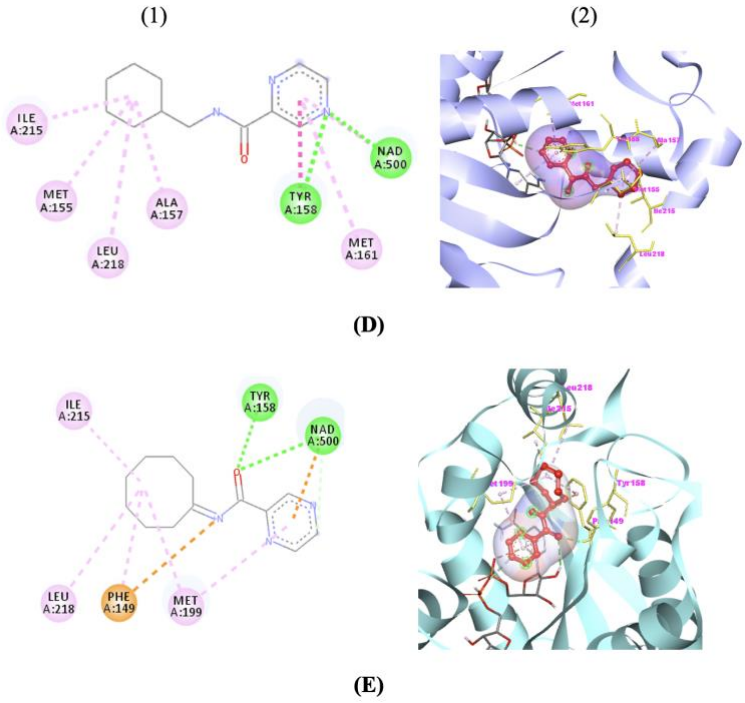

Figure 4. (1) 2D binding interaction (2) 3D binding interaction of compound **(D)** and **(E)** with ligands receptor 4TZK

The journal homepage www.jpacr.ub.ac.id
p-ISSN : 2302 – 4690 | e-ISSN : 2541 – 0733

CONCLUSION

Two pyrazine-2-carboxylic acid derivatives, *N*-(cyclohexylmethyl)pyrazine-2-carboxamide **(D)** and *N*-(4-cyclooctyl)pyrazine-2-carboxamide **(E)**, were successfully carried out by employing Yamaguchi reaction with yield of 60% and 55%, in respectively. *In silico* ADME and pharmacokinetic analysis revealed favorable drug-like properties, such as high gastrointestinal absorption, good solubility, and favorable membrane permeability. Both compounds were predicted to cross the blood-brain barrier, with compound (E) selectively inhibiting CYP1A2. Molecular docking studies showed that compounds **(D)** and **(E)** possessed better binding affinity, in comparison with standard drugs. The best activity was shown by *N*-(cyclohexylmethyl)pyrazine-2-carboxamide **(D)** with value of -7.65 kcal/mol. Future research should validate these predictions experimentally, through *in vitro* and *in vivo* studies, to assess the compounds' pharmacological efficacy, safety, and toxicity. Additionally, further structural modifications may enhance their therapeutic potential and minimize side effects, advancing them towards clinical trials for tuberculosis treatment.

ACKNOWLEDGMENT

The authors express their gratitude to the Directorate of Research, Technology, and Community Service (DRTPM) of the Ministry of Education, Culture, Research, and Technology (KEMDIKBUDRISTEK) for funding this research in 2024 under the scope of the Beginner Lecturer Research Program (Penelitian Dosen Pemula, PDP).

REFERENCES

[1] Niculescu, A. G., Mük, G. R., Avram, S., Vlad, I. M., Limban, C., Nuta, D., Grumezescu, A. M., and Chifiriuc, M. C., *Eur. J. Med. Chem.,* **2024**, 269, 116268.
[2] WHO, *Global Tuberculosis Report 2023*, https://www.who.int/teams/global-tuberculosis-programme/tb-reports/global-tuberculosis-report-2023/ Accessed 25 March 2024.
[3] Abdel-Aziz, M., and Abdel-Rahman, H. M. A., *Eur. J. Med. Chem.,* **2010**, 45 (8), 3384–3388.
[4] Wu, S.; Lan, L., Jiang, J., Ding, X., Ho, C. M., Lou, Y., Fan, G., *J. Pharm. Biomed. Anal.,* **2019**, 168, 44–54.
[5] Doležal, M.; Zitko, J., Kešetovičová, D., Kuneš, J., and Svobodová, M., *Molecules,* **2009**, 14 (10), 4180–4189.
[6] Semelkova, L., Konecna, K., Paterova, P., Kubicek, V., Kunes, J., Novakova, L., Marek, J., Naesens, L., Pesko, M., Kralova, K., Dolezal, M., and Zitko, J., *Molecules* **2015**, 20 (5), 8687–8711.
[7] Bouz, G., Semelková, L., Jand'ourek, O., Konečná, K., Paterová, P., Navrátilová, L., Kubíček, V., Kuneš, J., Doležal, M., and Zitko, J., *Molecules,* **2019**, 24 (7). 1212.
[8] Hosseini, S., Monajjemi, M., Rajaeian, E., and Haghgu, M., *Iran J. Pharm. Res.*, **2013**, 12 (4), 745–750.
[9] Zhang, Y., Wade, M. M., Scorpio, A., Zhang, H., and Sun, Z., *J. Antimicrob. Chemother.* **2003**, 52 (5), 790–795.
[10] Zhou, S., Yang, S., and Huang, G., *J. Enzyme Inhib. Med. Chem.,* **2017**, 32 (1), 1183–1186.
[11] Zitko, J., Jampilek, J., Dobrovolný, L., Svobodova, M., Kuneš, J., and Doležal, M., *Bioorganic Med. Chem. Lett.,* **2012**, 22 (4), 1598–1601.
[12] Krause, M., Foks, H., Augustynowicz-Kopeć, E., Napiórkowska, A., Szczesio, M., and

The journal homepage www.jpacr.ub.ac.id
p-ISSN : 2302 – 4690 | e-ISSN : 2541 – 0733

Gobis, K., *Molecules* **2018**, 23 (4), 1–15.
[13] Gobis, K., Foks, H., Serocki, M., Augustynowicz-Kopeć, E., Napiórkowska, A., *Eur. J. Med. Chem.,* **2015**, 89, 13–20.
[14] Zulqurnain, M., Aijijiyah, N. P., Wati, F. A., Fadlan, A., Azminah, A., and Santoso, M., *J. Appl. Pharm. Sci.,* **2023**, 13 (11), 170–177.
[15] Onajole, O. K., Pieroni, M., Tipparaju, S. K., Lun, S., Stec, J., Chen, G., Gunosewoyo, H., Guo, H., Ammerman, N. C., Bishai, W. R., and Kozikowski, A. P., *J. Med. Chem.,* **2013**, 56 (10), 4093–4103.
[16] Zitko, J., Servusová, B., Paterová, P., Mandíková, J., Kubíček, V., Kučera, R., Hrabcová, V., Kuneš, J., Soukup, O., and Doležal, M., *Molecules,* **2013**, 18 (12), 14807–14825.
[17] Zulqurnain, M., Ghulam Fahmi, M. R., Fadlan, A., Santoso, M., *IOP Conf. Ser. Mater. Sci. Eng.,* **2020**, 833 (1), 6.
[18] Daina, A., Michielin, O., and Zoete, V. *Sci. Rep.* **2017**, *7*, 1–13.
[19] Morris, G. M., Huey, R., Lindstrom, W., Sanner, M. F., Belew, R. K., Goodsell, D. S., and Olson, A. J., *J. Comput. Chem.,* **2009**, 30 (16), 2785–2791.
[20] Inanaga, J., Hirata, K., Saeki, H., Katsuki, T., and Yamaguchi, M., *Bulletin of the Chemical Society of Japan*, **1979**, 52 (7), 1989–1993.
[21] Kawanami, Y., Dainobu, Y., Inanaga, J., Katsuki, T., and Yamaguchi, *Bull. Chem. Soc. Jpn.,* **1981**, 54 (3), 943–944.
[22] Angelova, V. T., Pencheva, T., Vassilev, N., K-Yovkova, E., Mihaylova, R., Petrov, B., and Valcheva, V., *Antibiotics,* **2022**, 11 (5), 1–22.
[23] Silva, A. M., Martins-Gomes, C., Ferreira, S. S., Souto, E. B., and Andreani, T., *Int. J. Mol. Sci.,* **2022**, 23 (15).
[24] Wu, D., Chen, Q., Chen, X., Han, F., Chen, Z., and Wang, Y., *Signal Transduct. Target. Ther.,* **2023**, 8 (1).
[25] Zhao, M., Ma, J., Li, M., Zhang, Y., Jiang, B., Zhao, X., Huai, C., Shen, L., Zhang, N., He, L., and Qin, S. *Int. J. Mol. Sci.,* **2021**, 22 (23), 1–16.
[26] Hallikeri, C. S., Patil, R., Kumar, S. R. P., Kulkarni, V. H., and Joshi, S. D., *Indian J. Heterocycl., Chem.,* **2020**, 30 (2), 223–232.
[27] Kumbar, S. S., Shettar, A., Joshi, S. D., and Patil, S. A., *J. Mol. Struct.,* **2021**, 1231, 130016.
[28] Infield, D. T., Rasouli, A., Galles, G. D., Chipot, C., Tajkhorshid, E., and Ahern, C. A. *J. Mol. Biol.,* **2021**, 433 (17), 167035.

The journal homepage www.jpacr.ub.ac.id
p-ISSN : 2302 – 4690 | e-ISSN : 2541 – 0733